

# UCLA

## UCLA Previously Published Works

### Title

Valosin-Containing Protein/p97 as a Novel Therapeutic Target in Acute Lymphoblastic Leukemia.

### Permalink

<https://escholarship.org/uc/item/33r8b6qq>

### Journal

Neoplasia (New York, N.Y.), 19(10)

### ISSN

1522-8002

### Authors

Gugliotta, Gabriele  
Sudo, Makoto  
Cao, Qi  
et al.

### Publication Date

2017-10-01

### DOI

10.1016/j.neo.2017.08.001

Peer reviewed

# Valosin-Containing Protein/p97 as a Novel Therapeutic Target in Acute Lymphoblastic Leukemia



Gabriele Gugliotta<sup>\*,†</sup>, Makoto Sudo<sup>‡</sup>, Qi Cao<sup>†</sup>, De-Chen Lin<sup>†,‡</sup>, Haibo Sun<sup>†</sup>, Sumiko Takao<sup>‡</sup>, Ronan Le Moigne<sup>§</sup>, Mark Rolfe<sup>§</sup>, Sigal Gery<sup>†</sup>, Markus Müschen<sup>¶</sup>, Michele Cavo<sup>\*</sup> and H. Phillip Koeffler<sup>†,‡,¶</sup>

<sup>\*</sup>Institute of Hematology “L. & A. Seràgnoli”, Department of Experimental, Diagnostic, and Specialty Medicine, University of Bologna, Bologna, Italy; <sup>†</sup>Department of Hematology and Oncology, Cedars-Sinai Medical Center, Los Angeles, CA, USA; <sup>‡</sup>Cancer Science Institute of Singapore, National University of Singapore, Singapore; <sup>§</sup>Cleave Biosciences, Inc., Burlingame, CA 94010, USA; <sup>¶</sup>Department of Laboratory Medicine, University of California, San Francisco, San Francisco, CA, USA; <sup>¶</sup>National University Cancer Institute of Singapore, National University Hospital, Singapore.

## Abstract

B acute lymphoblastic leukemia (B-ALL) cells are distinctively vulnerable to endoplasmic reticulum (ER) stress. Recently, inhibition of p97 was shown to induce ER stress and subsequently cell death in solid tumors and in multiple myeloma. We investigated the role of a novel, orally available, p97 inhibitor (CB-5083; Cleave Biosciences) in B-ALL. CB-5083 induced a significant reduction in viability in 10 human B-ALL cell lines, harboring the most common fusion-genes involved in pediatric and adult B-ALL, with IC50s ranging from 0.34 to 0.76  $\mu$ M. Moreover, CB-5083 significantly reduced the colony formation of OP1 and NALM6 cells. Early and strong induction of apoptosis was demonstrated in BALL1 and OP1 cells, together with a robust cleavage of PARP. CB-5083 induced ER stress, as documented through: 1) prominent expression of chaperones (GRP78, GRP94, PDI, DNAJC3, and DNAJB9); 2) increased activation of IRE1- $\alpha$ , as demonstrated by the splicing of XBP1; and 3) activation of PERK, which resulted in a significant overexpression of CHOP, and its downstream genes. CB-5083 reduced the viability also in GRP78<sup>-/-</sup>, GRP94<sup>-/-</sup>, and XBP1<sup>-/-</sup> cells, suggesting that none of these proteins alone was strictly required for CB-5083 activity. Moreover, we showed that the absence of XBP1 (XBP1<sup>-/-</sup>) increased the sensitivity to CB-5083, leading to the hypothesis that XBP1 splicing counteracts the activity of CB-5083, probably mitigating ER stress. Finally, vincristine was synergistic with CB-5083 in both BALL1 and OP1 cells. In summary, the targeting of p97 with CB-5083 is a novel promising therapeutic approach that should be further evaluated in B-ALL.

*Neoplasia* (2017) 19, 750–761

## Introduction

### Acute Lymphoblastic Leukemia

In the United States each year, approximately 6000 patients are diagnosed with acute lymphoblastic leukemia (ALL) [1]; half of these are adults. Survival rate in children and adolescents has increased from less than 10% in the 1960s to 90% today [1], but these results are not replicated in adults [2]. Indeed, the long-term overall survival in adults is only 30% to 40% for those younger than 60 years and less than 10% for those older than 60 years [3,4]. Therefore, new treatment options are clearly needed in these patients; and recent efforts have introduced targeted therapies that focus on specific

Abbreviations: B-ALL, B acute lymphoblastic leukemia; ER, endoplasmic reticulum; UPR, unfolded protein response; ERAD, ER-associated degradation; MTT, 3-(4,5-dimethylthiazol-2-yl)-2,5-diphenyltetrazolium bromide; HNA, 2-hydroxy-1-naphthaldehyde; PI, propidium iodide; PEI, polyethylenimine; 4-OHT, 4-hydroxy tamoxifen

Address all correspondence to: Gabriele Gugliotta, M.D., Ph.D., Institute of Hematology “L. & A. Seràgnoli”, Department of Experimental, Diagnostic, and Specialty Medicine, University of Bologna, Via Massarenti 9, 40138, Bologna, Italy. E-mails: [gabriele.gugliotta@unibo.it](mailto:gabriele.gugliotta@unibo.it)

Received 9 July 2017; Revised 4 August 2017; Accepted 4 August 2017

© 2017 The Authors. Published by Elsevier Inc. on behalf of Neoplasia Press, Inc. This is an open access article under the CC BY-NC-ND license (<http://creativecommons.org/licenses/by-nc-nd/4.0/>). 1476-5586

<http://dx.doi.org/10.1016/j.neo.2017.08.001>

weaknesses of ALL cells [5]. In this context, B-ALL cells were recently noted to be distinctively vulnerable to endoplasmic reticulum (ER) stress, identifying the unfolded protein response (UPR) as a novel therapeutic target in acute leukemia [6,7].

**ER Stress and Unfolded Protein Response**  
The ER is an intracellular organelle with fundamental functions in the secretory pathway, including translocation, folding, and posttranslational modifications of proteins. The ER stress refers to those conditions that

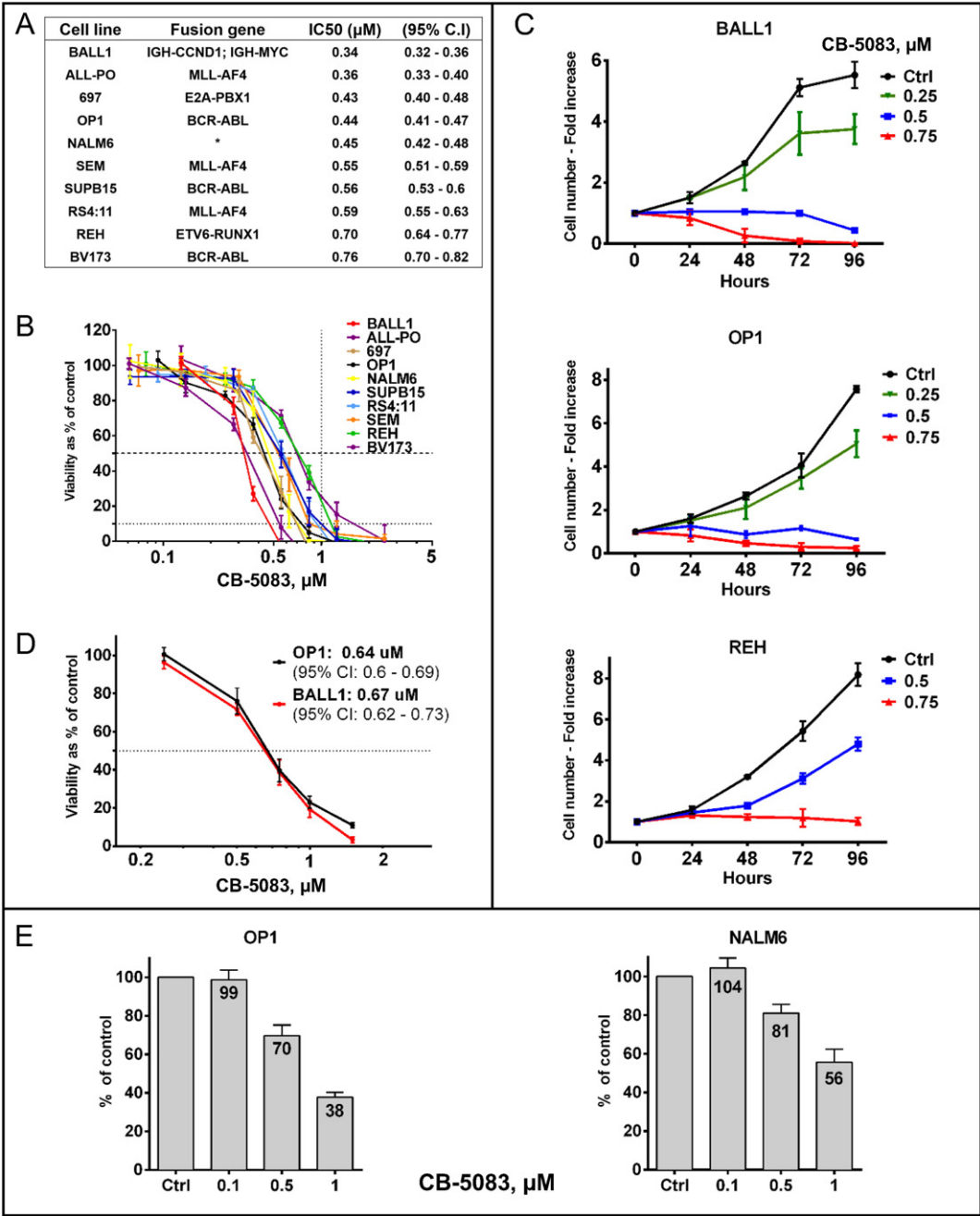


**Figure 1.** Evaluation of viability, proliferation, and clonogenic potential of B-ALL cell lines treated with CB-5083. (A) Fusion genes associated with 10 human B-ALL cell lines treated with CB-5083, and their corresponding IC50s (mean, and 95% confidence intervals, CIs). For each cell line, viability was measured at 72 hours by MTT assays (3 experiments, each in triplicates). \*: t(5;12)(q31q33; p12), which is not associated with usual fusion genes in B-ALL. (B) MTT assays of the 10 B-ALL cell lines treated with CB-5083: viability measured at 72 hours expressed as % of control (vehicle – DMSO); mean ± SD of three experiments in triplicates for each cell line. (C) Proliferation assays of three cell lines (BALL1, OP1, and REH) treated with different concentrations of CB-5083 for various durations. Viable cells were counted at 24, 48, 72, and 96 hours (trypan blue exclusion). Experiments (*n* = 3) were done in duplicates; proliferation is expressed as fold changes (mean ± SD) compared to baseline (=1). (D) MTT assays of two cell lines (BALL1 and OP1): viability measured at 24 hours expressed as % of control (vehicle – DMSO); mean ± SD of three experiments in triplicates for each cell line. (E) Colony assays in methyl-cellulose of the OP1 and NALM6 cells: cells were plated in methyl-cellulose in the presence of different concentrations of CB-5083, and the resulting colonies (OP1, at 15 days; NALM-6, at 12 days) were counted. Experiments (*n* = 3) were done in duplicates, and the number of colonies in experimental wells is expressed as % (mean [numbers in the boxes] ± SD) of colonies in the diluent control.

affect ER function. Under ER stress, the cell activates UPR, a complex system that tries to restore protein homeostasis by increasing expression of ER chaperones, reducing the protein loading to ER through inhibition of mRNA translation, and promoting ER-associated degradation (ERAD) [8]. If these adaptive mechanisms fail, UPR is able to activate pathways leading to apoptosis [9]. UPR takes place through three different branches in which the signaling is initially mediated by IRE1- $\alpha$  (inositol-requiring protein-1  $\alpha$ ), PERK (Protein kinase RNA-like ER kinase), and ATF6 (activating transcription factor 6). The chaperone GRP78 (BIP) is the main sensor of ER stress. Under physiological conditions, it binds IRE1- $\alpha$ , PERK, and ATF6, preventing their activation. However, in the presence of excess of unfolded proteins (higher levels of ER stress), GRP78 binds to these unfolded proteins and dissociates from IRE1- $\alpha$ , PERK, and ATF6, resulting in their activation.

### p97 and ERAD

Valosin-containing protein, p97 (VCP/p97, Cdc48 in yeast) [10] is an abundant, conserved ATPase involved in diverse cellular activities, including ERAD, chromatin-associated degradation, mitochondria-associated degradation, and autophagy [11–13]. ERAD requires the retrograde (from ER to cytoplasm) transportation of unfolded proteins, which are ultimately destroyed by the ubiquitin-proteasome system. The activity of the p97 protein in ERAD is mediated by the formation of a complex with two co-factors: ubiquitin fusion-degrading protein 1 (Ufd1) and nuclear protein localization protein 4 homolog (Npl4). The p97-Ufd1-Npl4 complex is recruited to the ER membrane, where it plays a fundamental role in the extraction of the protein from the ER lumen to the cytosol. Loss of p97 ATPase activity blocks proteasomal degradation of several different ERAD substrates [11].

Pharmacological inhibition of p97 induces ER stress and subsequently cell death in solid tumors [14,15] and in multiple myeloma [15], with promising activity and tolerability in *in vivo* models. On that basis, two phase I clinical trials with a novel, orally available, p-97 inhibitor CB-5083 (Cleave Biosciences) [15,16] have been initiated in these settings (ClinicalTrials.gov: NCT02243917 and NCT02223598). However, no data are available on effects of the inhibition of p97 in B-ALL. For these reasons, we investigated the role of CB-5083 in B-ALL models.

## Methods

Detailed methods are described in the supplemental material.

### Cell Lines

The following human B-ALL cell lines were used: BALL1, REH, NALM6, OP1, ALL-PO, 697, RS4;11, BV173, SEM, and SUPB15. OP1 cells were generously provided by Dario Campana (National University Cancer Institute, Singapore). ALL-PO cells were generously provided by Andrea Biondi (University of Milan-Bicocca, Monza, Italy). Murine BCR-ABL transformed B-ALL cell lines with floxed alleles (XBP1<sup>FL/FL</sup>, GRP78<sup>FL/FL</sup>, or GRP94<sup>FL/FL</sup>) were used.

### Viability Assay and Evaluation for Synergy

Cell viability was evaluated by 3-(4,5-dimethylthiazol-2-yl)-2,5-diphenyltetrazolium bromide (MTT) assay. Half maximal inhibitory concentrations (IC50s) were calculated using the GraphPad Prism 6 software. For pulse exposure assays, cells were treated with CB-5083 for the desired interval, washed three times with phosphate buffer saline (PBS), and seeded with fresh media, and viability was evaluated by MTT assay.

For drug combination assays, cells were seeded in 96-well plates, followed by addition of either vehicle or increasing

concentrations of CB-5083 alone, second drug (vincristine, bortezomib, 2-hydroxy-1-naphthaldehyde [HNA], or prednisolone) alone, or CB-5083 plus second drug. Viability was evaluated by MTT assay as previously described. Synergistic combination of two drugs was determined using the CompuSyn software. The extent of drug interaction between the two drugs was determined using the combination index (CI) for mutually exclusive drugs. CI values were obtained when solving the equation for different concentrations of drugs. A CI of 1 indicates an additive effect, whereas a CI of <1 denotes synergy.

### Cell Proliferation and Clonogenic Assay

Cell proliferation was evaluated with trypan blue exclusion. For clonogenic assay, either NALM-6 or OP1 cells were grown in methyl-cellulose (Methocult H4230, STEMCELL Technologies). Colonies were counted under an inverted microscope after either 12 (NALM6) or 15 days (OP1).

### Apoptosis and Cell Cycle Analysis

Apoptosis was determined by Annexin V/PI staining (BD Biosciences) according to manufacturer's instructions. Cell cycle analyses were performed by propidium iodide staining (Sigma-Aldrich) for DNA content and flow cytometric analysis. All flow cytometry data were analyzed using FlowJo software (Tree Star, Ashland, OR).

### Western Blotting and PCR

Western blotting and PCR were performed as previously described [7], following standard procedures.

### Retroviral Transduction and Inducible Knockout

Retroviral constructs and the corresponding empty vector controls were packaged in Platinum-E (Plat-E) cells using polyethylenimine (PEI) transfection method. Nine micrograms of plasmid (either MSCV-ER<sup>T2</sup> or MSCV-Cre-ER<sup>T2</sup>) was incubated with 27  $\mu$ l of PEI reagent (1  $\mu$ g/ $\mu$ l) in 1000  $\mu$ l Opti-MEM media (Invitrogen) for 20 minutes. The mixture was placed on the Plat-E cells in 10-cm culture dishes. The virus supernatants were harvested 24 and 48 hours later. Viral supernatants from two collections were combined, filtered through a 0.45- $\mu$ m filter, and loaded on RetroNectin (Clontech)-coated nontissue 6-well plates, and  $2 \times 10^6$  cells (BCR-ABL+ B-ALL GRP78<sup>FL/FL</sup>, GRP94<sup>FL/FL</sup>, or XBP1<sup>FL/FL</sup>) per well were transduced following the manufacturer's instructions. These transduced cells were selected for 48 to 72 hours with puromycin (1–2  $\mu$ M). CRE-mediated deletion of GRP78, GRP94, or XBP1 was accomplished by treatment of these cells with 4-OHT (1  $\mu$ M) for 2 days.

### Statistical Analysis

IC50s are expressed as mean and 95% confidence intervals. All other results are expressed as mean  $\pm$  SD. Statistical significance was determined by Student's *t* test or one-way ANOVA, as appropriate. Significance of *P* values less than .05, .01, .001, and .0001 is shown with \*, \*\*, \*\*\*, and \*\*\*\* asterisks, respectively.

## Results

### Viability, Proliferation, and Colony Assay

CB-5083 was tested against a panel of 10 human B-ALL cell lines harboring the most common fusion genes involved in pediatric and adult B-ALL [17] (Figure 1A). Viability after 72 hours of treatment



with CB-5083 at different concentrations was evaluated with MTT assays ( $n = 3$ ). CB-5083 demonstrated robust activity against all the cell lines, with IC50s ranging from 0.34  $\mu\text{M}$  (BALL1) to 0.76  $\mu\text{M}$  (BV173) (Figure 1, A and B). Moreover, the IC90s were below 1  $\mu\text{M}$  in 8/10 tested cell lines (exception was REH and BV173) (Figure 1B).

Further, the proliferation of BALL1, OP1, and REH cells exposed to different CB-5083 concentrations was evaluated by trypan blue exclusion at 24, 48, 72, and 96 hours (Figure 1C). At 96 hours, treatment with CB-5083 (0.5  $\mu\text{M}$  and 0.75  $\mu\text{M}$ ) significantly reduced the number of viable cells compared to untreated cells (fold changes with respect to baseline are reported in Supplemental Table 1). Of note, treatment of BALL1 and OP1 with CB-5083 0.75  $\mu\text{M}$  significantly lowered the number of viable cells compared to baseline, suggesting a cytotoxic activity of CB-5083, which was already pronounced at 48 hours; in REH cells, at 0.75  $\mu\text{M}$ , the number of viable cells remained almost unchanged, suggesting a cytostatic activity. The rapid activity of CB-5083 was confirmed by MTT assays after a short exposure (24 hours) to the drug, with an IC50s of 0.68  $\mu\text{M}$  and 0.64  $\mu\text{M}$  for BALL1 and OP1 cells, respectively (Figure 1D).

We then evaluated the clonogenic potential of B-ALL cells under continuous exposure to the drug (Figure 1E). Colonies of NALM6 and OP1 were grown in methyl-cellulose under different drug concentrations (0.1, 0.5, and 1  $\mu\text{M}$ ). CB-5083 was not effective at the lowest concentration tested (0.1  $\mu\text{M}$ ). In cells treated with higher concentrations, a significant reduction occurred in the number of colonies (% decreased compared to control [untreated cells]; mean  $\pm$  SD): OP1, 70% ( $\pm 5.5$ ) and 38% ( $\pm 2.5$ ) at 0.5  $\mu\text{M}$  and 1  $\mu\text{M}$ , respectively; NALM6, 81% ( $\pm 4.6$ ) and 56% ( $\pm 6.6$ ) at 0.5  $\mu\text{M}$  and 1  $\mu\text{M}$ , respectively. Moreover, after treatment with 1  $\mu\text{M}$ , colonies appeared smaller compared to control (morphologic observation, data not shown).

### Apoptosis and Cell Cycle

To confirm the cytotoxic activity of CB-5083, we evaluated the rates of apoptosis at 24, 48, and 72 hours after treatment with CB-5083 (0.25, 0.5, and 0.75  $\mu\text{M}$ ). Apoptosis was measured by flow cytometry, after staining with Annexin V and propidium iodide, in BALL1 (Figure 2) and OP1 (Supplemental Figure 1). CB-5083 induced apoptosis in both cell lines. For BALL1, at 24 hours, the proportion of apoptotic cells was significantly higher in treated (0.75  $\mu\text{M}$ : 54%; 0.5  $\mu\text{M}$ : 29%) versus control cells (14%;  $P < .0001$ , and  $P = .02$ , respectively); the degree of apoptosis increased at later time points and was massive at 72 hours (0.75  $\mu\text{M}$ : 94%; 0.5  $\mu\text{M}$ : 71%; control: 15%;  $P < .0001$  for both comparisons). A similar trend, although to a lower degree, was found also for OP1 (Supplemental Figure 1).

By Western blot (Figure 3, A and B), we showed a significant cleavage of PARP1 in BALL1 and OP1 cells as early as 8 hours of treatment; cleaved PARP was documented even at 24 hours in cells treated with CB-5083 (0.75  $\mu\text{M}$ ).

Cell cycle analysis was performed (Figure 4); considering that marked rates of apoptosis were observed at 24 hours, we investigated the effects on the cell cycle at an earlier exposure (12 hours) of CB-5083 but at a higher dose (1  $\mu\text{M}$ ). Compared to control, for both BALL1 and OP1, a significant difference did not occur in the percentage of cells with  $>2\text{N}$  DNA content, suggesting that cells already in S phase were able to continue to the G2/M phase. On the contrary, a significantly lower number of cells with  $2\text{N}$  DNA content (diploid) were noted, associated with a proportional increase of cells with  $<2\text{N}$  DNA content (sub-G1; apoptotic cells). These findings

suggest that cells may enter the apoptotic process from the G1 phase. In detail for BALL1, treated versus control,  $2\text{N}$  cells: 38% versus 50% ( $P = .003$ );  $<2\text{N}$  cells: 21% versus 5% ( $P = .008$ ). For OP1, treated versus control,  $2\text{N}$  cells: 41% versus 56% ( $P = .0007$ );  $<2\text{N}$  cells: 29% versus 12% ( $P = .005$ ).

### Pulse Exposure

Since CB-5083 reduced viability and induced apoptosis by 12 to 24 hours of treatment, we investigated the cytotoxic activity of CB-5083 in BALL1, OP1, and REH cells after pulse exposure: treatment of target cells for shorter durations (4 and 8 hours) but at higher doses (1  $\mu\text{M}$  and 2.5  $\mu\text{M}$ ) (Supplemental Figures 2 and 3). After treatment with either vehicle or CB-5083 at the indicated doses and intervals, cells were rigorously washed with PBS and seeded in new media. Viability was evaluated at 72 hours with MTT assays. Pulse exposure to CB-5083 (1  $\mu\text{M}$  for 4 or 8 hours, or 2.5  $\mu\text{M}$  for 4 hours) had little effect. In contrast, 2.5  $\mu\text{M}$  drug pulse exposure for 8 hours significantly reduced viability at 72 hours. Moreover, 2.5  $\mu\text{M}$  drug pulse exposure for 8 hours significantly increased the rate of apoptosis of BALL1 and OP1 cells at 24 hours.

### Induction of ER Stress

As markers of ER stress, we investigated the activation of IRE1-alpha and PERK pathways, and the synthesis of chaperones of BALL1, OP1, and REH cells exposed to CB-5083 at different concentrations and durations.

**IRE1-alpha and XBP1 Splicing.** Western blot showed dose-dependent increased levels of IRE1-alpha in the BALL1 and OP1 cells treated with CB-5083 (0.25, 0.5, and 0.75  $\mu\text{M}$ ; 24 hours) (Figure 3C). Increase in IRE1-alpha in BALL1 appeared as early as 4 hours from exposure to CB-5083 (1  $\mu\text{M}$ ) (Supplemental Figure 4). The activation of IRE1-alpha was confirmed by the demonstration of the splicing of XBP1 into the short-form sXBP1 in the three cell lines (BALL1, OP1, and REH) (Figure 5A). The XBP1 splicing was strongly induced in BALL1: sXBP1 appeared early by 4 hours at 0.5  $\mu\text{M}$  of drug and was maximum at 8 hours with higher CB-5083 concentrations (2.5 and 5  $\mu\text{M}$ ). XBP1 splicing occurred also in REH cells, although with lower intensity, after exposure to higher doses of drug (2.5 and 5  $\mu\text{M}$ ). OP1 showed an intermediate degree of XBP1 splicing between BALL1 and REH.

**PERK and CHOP.** For BALL 1 and OP1 cells treated with CB-5083 (0.25, 0.5, and 0.75  $\mu\text{M}$ ; 24 hours), Western blot showed increased levels of PERK compared to control, suggesting its increased expression (Figure 3C). PERK plays an essential role in the attenuation of mRNA translation (adaptive response). CHOP is an activator of apoptosis following ER stress. Increased expression of CHOP by CB-5083 was demonstrated at the protein level by Western blot (Figure 3A). Levels of CHOP mRNA measured by Q-PCR in BALL1, OP1, and REH after a short exposure (4 and 8 hours) of CB-5083 (0.5, 1, 2.5, 5  $\mu\text{M}$ ) showed that CHOP expression significantly increased as early as 4 hours from exposure to the drug at its lowest concentration for all the cell lines (Figure 5B). CHOP expression increased proportionally with higher doses and longer exposures, reaching the highest levels at 8-hour culture with 5  $\mu\text{M}$  of the drug: 67-, 34-, and 54-fold higher levels than the control in BALL1, OP1, and REH cells, respectively.

Other genes (GADD34, DR5, ATF4, and caspase-2) potentially involved in the death process triggered by an irresolvable ER stress were also examined (Figure 5C). Treatment of BALL1 and OP1 with

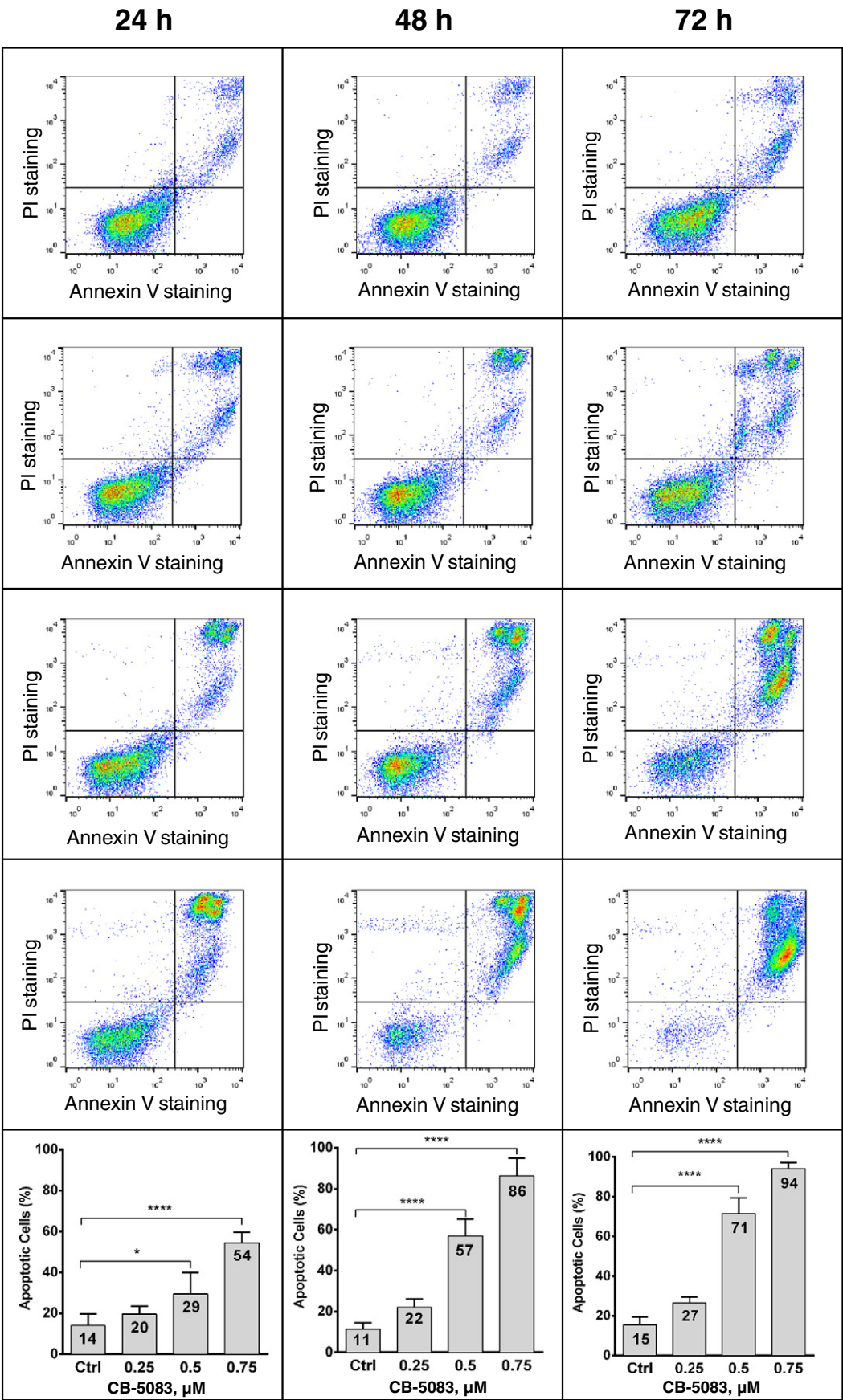


**Figure 2.** Apoptosis of BALL1 cells after treatment with CB-5083. Apoptosis was measured (Annexin V + propidium iodide positivity) after treatment with CB-5083 (0.25, 0.5, and 0.75 μM) for 24, 48, and 72 hours. Lower panels: bar graph quantification of data (mean [numbers in the boxes] ± SD of three experiments; ANOVA: all  $P < .0001$ ; \*:  $P < .05$ ; \*\*\*\*:  $P < .0001$ ).

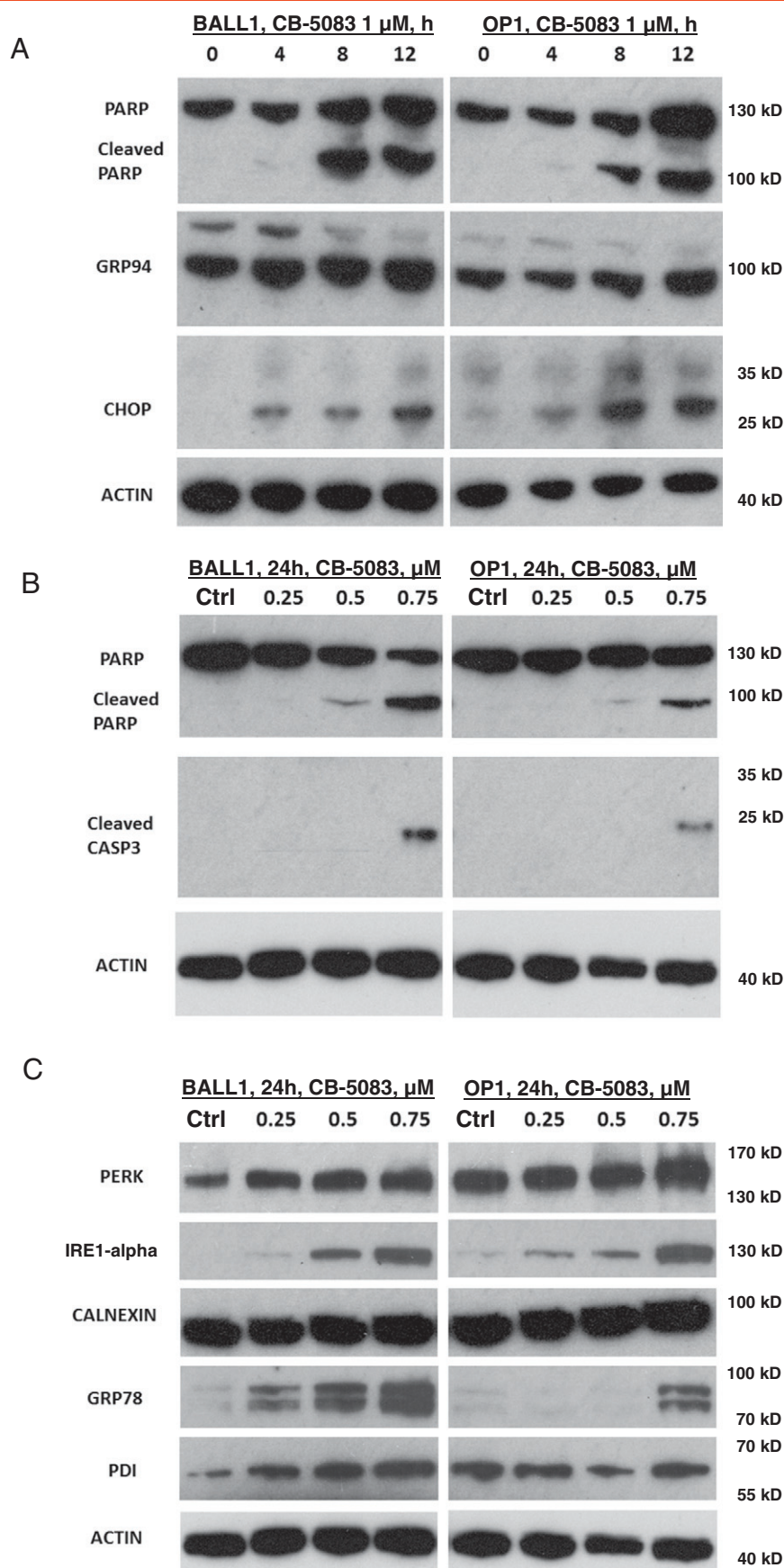


**Figure 3.** Protein expression of ER stress markers and PARP cleavage as determined by Western blot in BALL1 and OP1 cells after treatment with CB-5083. Cells were treated with CB-5083 at a fixed dose (1  $\mu$ M) for the indicated time (A), as well as for 24 hours at the indicated CB-5083 concentrations (B and C). Western blots were probed with a series of antibodies directed against PERK, IRE1-alpha, calnexin, GRP78, GRP94, PDI, CHOP, PARP, and cleaved caspase-3.  $\beta$ -Actin was used as a loading control.



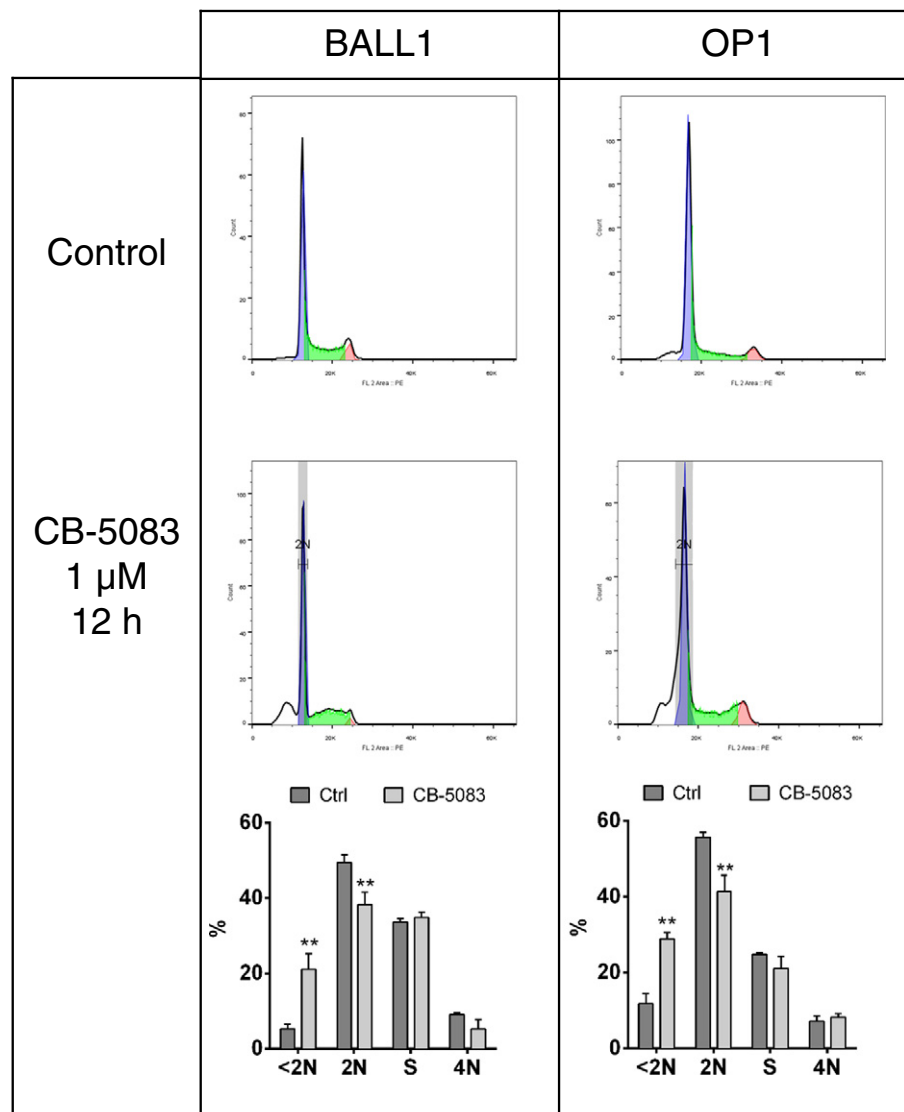


**Figure 4.** Cell cycle analysis in BALL1 and OP1 cells after treatment with CB-5083. Cell cycle analysis of BALL1 and OP1 after treatment with CB-5083 (1  $\mu$ M, 12 hours). Staining was performed with propidium iodide. CTRL, diluent control. Quantification of data (mean  $\pm$  SD of three experiments) provided in bottom panels. \*\*:  $P < .01$ .

CB-5083 (5  $\mu$ M; 8 hours) induced a significant increase of GADD34 mRNA expression (11.5- and 9.4-fold compared to control in BALL1 and OP1 cells, respectively), a downstream target of CHOP, reinforcing the concept that this mechanism plays an important role in inducing apoptosis in B-ALL cells. A slightly higher mRNA expression compared to control was also found for DR5 (3.4- and 4.5-fold compared to control in BALL1 and OP1, respectively), ATF4 (3.2- and 2.6-fold compared to control in BALL1 and OP1, respectively), and caspase 2 (2.3- and 3.2-fold compared to control in BALL1 and OP1, respectively).

**Chaperones.** For BALL1 and OP1 cells treated with CB-5083 (0.25, 0.5, and 0.75  $\mu$ M for 24 hours, as well as 1  $\mu$ M for 4, 8, and 12 hours), Western blot demonstrated increased levels of GRP78, GRP94, and PDI proteins, while no significant increase of calnexin, another marker of ER stress, occurred (Figure 3, A and C). CB-5083 (5  $\mu$ M, 8 hours) also increased expression of GRP78 mRNA (6.9- and 9.1-fold) and GRP94 mRNA (7.4- and 5.6-fold) compared to control in BALL1 and OP1 cells, respectively (Figure 5C). Moreover,

CB-5083 (5  $\mu$ M, 8 hours) significantly increased expression of two other chaperones, DNAJC3 mRNA (8.7- and 7.5-fold) and DNAJB9 mRNA (9.3- and 13.7-fold), compared to control in BALL1 and OP1 cells, respectively (Figure 5C).

#### Knockdown of XBP1, GRP78, and GRP94

Given the higher expression of GRP78 and GRP94 and the increased splicing of XBP1 after treatment with CB-5083, effect of the drug was also examined when each of these genes was deleted. We used murine B cells with floxed alleles (GRP78<sup>FL/FL</sup>; GRP94<sup>FL/FL</sup>; XBP1<sup>FL/FL</sup>) transfected with the BCR-ABL oncogene (p190 for GRP78<sup>FL/FL</sup> and GRP94<sup>FL/FL</sup>; P210 for XBP1<sup>FL/FL</sup>) as models of BCR-ABL+ B-ALL. These BCR-ABL+ B-ALL floxed cells were transfected with either an empty vector (EV) or estrogen-inducible CRE-recombinase, selected with puromycin, and treated with 4-hydroxy-tamoxifen (4-OHT), resulting in EV-GRP78<sup>+/+</sup>; EV-GRP94<sup>+/+</sup>; and EV-XBP1<sup>+/+</sup> cells or in CRE-GRP78<sup>-/-</sup>; CRE-GRP94<sup>-/-</sup>; and CRE-XBP1<sup>-/-</sup> cells (knockdown cells).



Viability of these cells was evaluated after treatment with 4-OHT (1  $\mu$ M) either alone (Supplemental Figure 5) or in combination with CB-5083 (various concentrations) (Figure 6).

In CRE-GRP78<sup>-/-</sup>, CRE-GRP94<sup>-/-</sup>, and CRE-XBP1<sup>-/-</sup>, CB-5083 significantly reduced viability at 72 hours compared to untreated cells, suggesting that the drug is effective even though these cells lack these genes. Moreover, we compared the relative (normalized to untreated cells) viability of CRE-XBP1<sup>-/-</sup>, CRE-GRP78<sup>-/-</sup>, and CRE-GRP94<sup>-/-</sup> versus EV-XBP1<sup>+/+</sup>, EV-GRP78<sup>+/+</sup>, and EV-GRP94<sup>+/+</sup> cells, respectively, during culture with CB-5083. In the absence of XBP1 (CRE-XBP1<sup>-/-</sup>), the viability after treatment with CB-5083 (0.3 – 0.4 – 0.5  $\mu$ M) was significantly lower compared to control (EV-XBP1<sup>+/+</sup>). In contrast, the viability after treatment with CB-5083 was not significantly changed by the absence of either GRP78 (CRE-GRP78<sup>-/-</sup>) or GRP94 (CRE-GRP94<sup>-/-</sup>) compared to control cells (EV-GRP78<sup>+/+</sup> and EV-GRP94<sup>+/+</sup>, respectively) (Figure 6).

Combination Studies

The potential synergy of CB-5083 with other drugs was tested. Firstly, the combination with drugs that represent the backbone of B-ALL treatment, vincristine and prednisolone, was examined. The combination of CB-5083 with vincristine for 24 hours was synergistic

(Figure 7), with combination indexes (CI) as low as 0.56 and 0.58 for BALL1 and OP1 cells, respectively. Prior data showed that high VCP/p97 expression correlated with poor prednisone response in B-ALL [18]. We found that the combination of CB-5083 plus prednisolone in two prednisolone-resistant cell lines (BALL1 and REH) did not show synergistic activity (restoration of steroid sensitivity) (Supplemental Figure 6). Other drugs inducing ER stress were studied; neither the proteasome inhibitor bortezomib nor the IRE1-alpha inhibitor HNA produced synergy with CB-5083 (Supplemental Figure 6).

Discussion

The present study showed that CB-5083, an orally available inhibitor of the ATPase p97/VCP [15,16], has antileukemic activity through the induction of ER stress using a wide panel of B-ALL cell lines, including those harboring the fusion genes most frequently found in adult and pediatric B-ALL [17]. We did not identify cell lines with upfront resistance to the drug, with IC50s ranging from 0.34 to 0.76  $\mu$ M. Importantly, these concentrations are attainable in mice, without significant toxicities [15]. Moreover, CB-5083 reduced the viability in murine models of BCR-ABL+ (p190 and p210) B-ALL, with IC50s comparable to those observed in human B-ALL cell lines. The sensitivity to CB-5083 of B-ALL cells regardless of their underlying

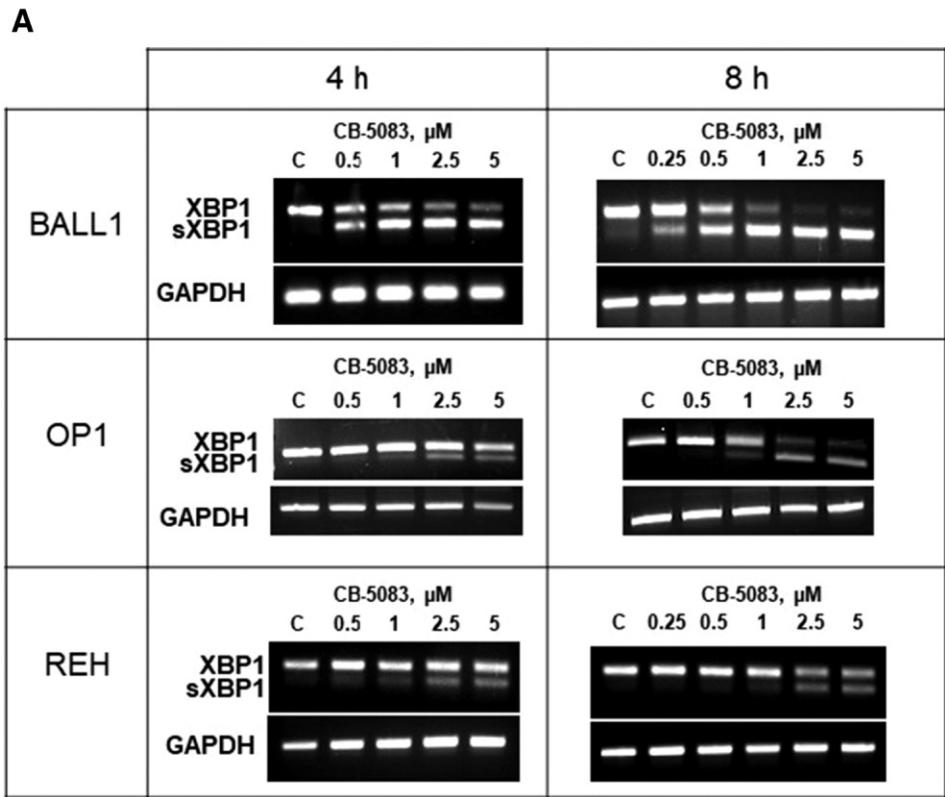


**Figure 5.** XBP1 splicing and expression of genes involved in ER stress after treatment with CB-5083. After treatment of three B-ALL cell lines (BALL1, OP1, REH) with either vehicle or CB-5083 at the indicated concentrations and intervals, mRNA was extracted, and XBP1 and spliced XBP1 (sXBP1) were evaluated with RT-PCR (35 cycles) (A). CHOP expression was measured by QRT-PCR (B). In BALL1 and OP1 cells treated for 8 hours with CB-5083 (5  $\mu$ M) versus diluent control, mRNA was isolated and used for QRT-PCR for genes involved in unfolded protein response and in death pathways (C). GAPDH mRNA was used as loading control (A). Quantitative gene expression data were normalized to the expression levels of GAPDH (B and C). Bar graphs represent mean (numbers in the boxes)  $\pm$  SD of three experiments, each in triplicates. Multiple comparisons tests of CHOP expression are provided in Supplemental Tables 2, 3 and 4. As positive controls, XBP1 splicing and CHOP expression were also evaluated in BALL1, OP1, and REH cells treated with the ER stress inducer thapsigargin (Supplemental Figure 7).

## B

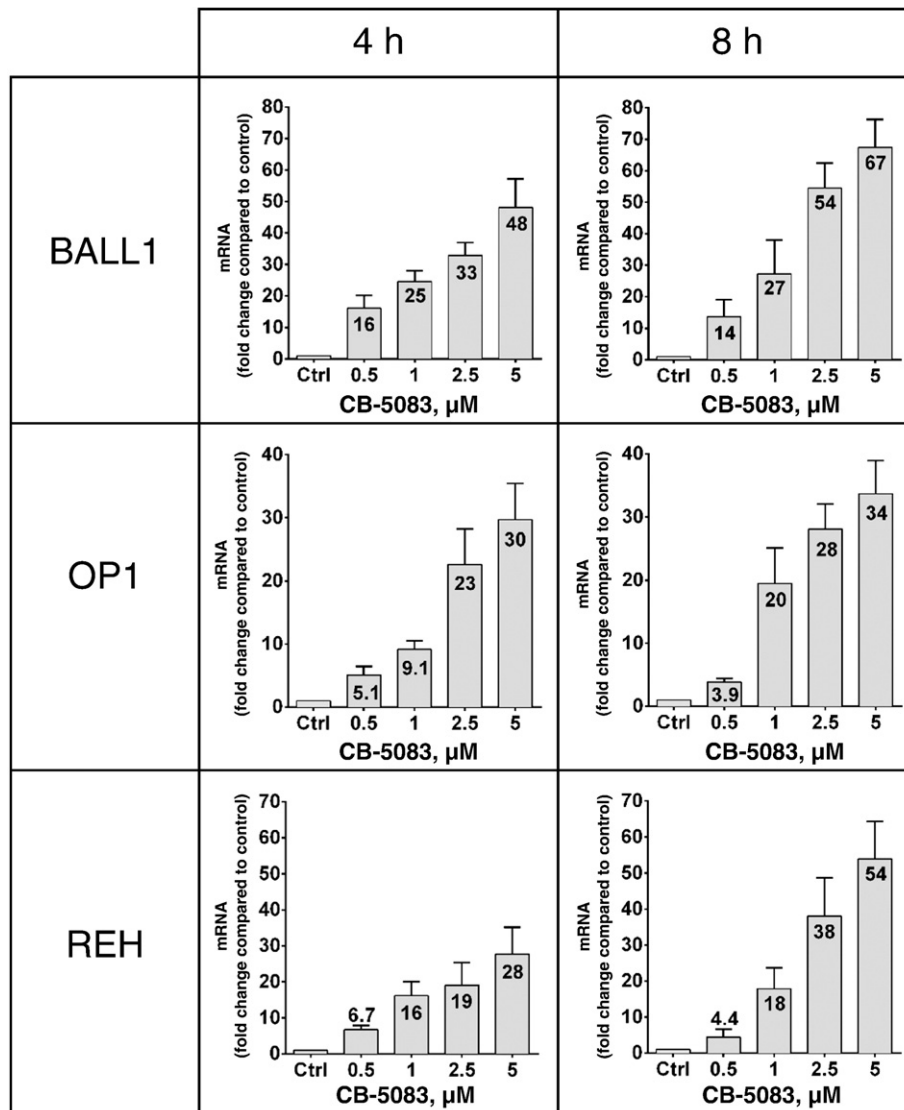


Figure 5. (continued.)

fusion gene can have interesting implications in the treatment of B-ALL with high-risk genetic alterations (MLL rearrangements; BCR-ABL+). Of note, the most sensitive B-ALL cell line (BALL1) harbors a translocation involving *c-myc*. *Myc*-driven tumorigenesis is associated with a high level of protein synthesis [19] and high levels of ER stress that trigger an adaptive UPR, required for cell survival and proliferation [20]. This finding reinforces the theory that CB-5083 might be particularly effective in cells heavily dependent on UPR for survival, as was demonstrated in multiple myeloma [15]. Moreover, this concept suggests that CB-5083 will be potent against tumors harboring *myc* translocations (e.g., Burkitt's lymphoma).

The proliferation assays highlighted that CB-5083, depending on the exposure and concentration, has both cytostatic and cytotoxic activity. The cytotoxicity was demonstrated by the induction of apoptosis, which increased with higher concentrations or longer exposures to the drug. Moreover, short exposure to high concentrations of the drug (pulse exposure), similar to peak concentrations reached *in vivo*, is enough to reduce the cell viability and to induce apoptosis.

The cell cycle analysis showed that CB-5083 significantly reduced the proportion of 2 N cells (G1 phase) and increased <2 N cells

(sub-G1; apoptotic) without affecting the proportion of >2 N cells (S phase) and 4 N cells (G2/M phase). The data suggest that these treated cells might enter into apoptosis during their G1 phase. These findings are consistent with the notion that B-ALL cells might be particularly susceptible to ER stress in G1 when, physiologically, a high burden of protein synthesis occurs and, consequently, a higher demand for efficient management of unfolded proteins.

The clonogenic experiments using OP1 and NALM6 cells confirmed the activity of CB-5083, with a significant reduction in the number of colonies after a continuous exposure to the drug. However, the antiproliferative effects were lower than expected because we still observed moderate clonogenic growth after treatment with 1  $\mu\text{M}$  CB-5083 (38% in OP1 and 56% in NALM6 compared to dishes containing diluent control). The cause could be multifactorial including that the half-life of the drug in methyl-cellulose is short. In this context, the sigmoidal shape and the steep slope of the concentration/viability curves observed for the cell lines suggest that small variations in CB-5083 concentration may cause dramatic changes in the potency of the drug.

Previously, ER stress and UPR were identified as therapeutic targets in B-ALL [6]. Here, we show that CB-5083 has a significant

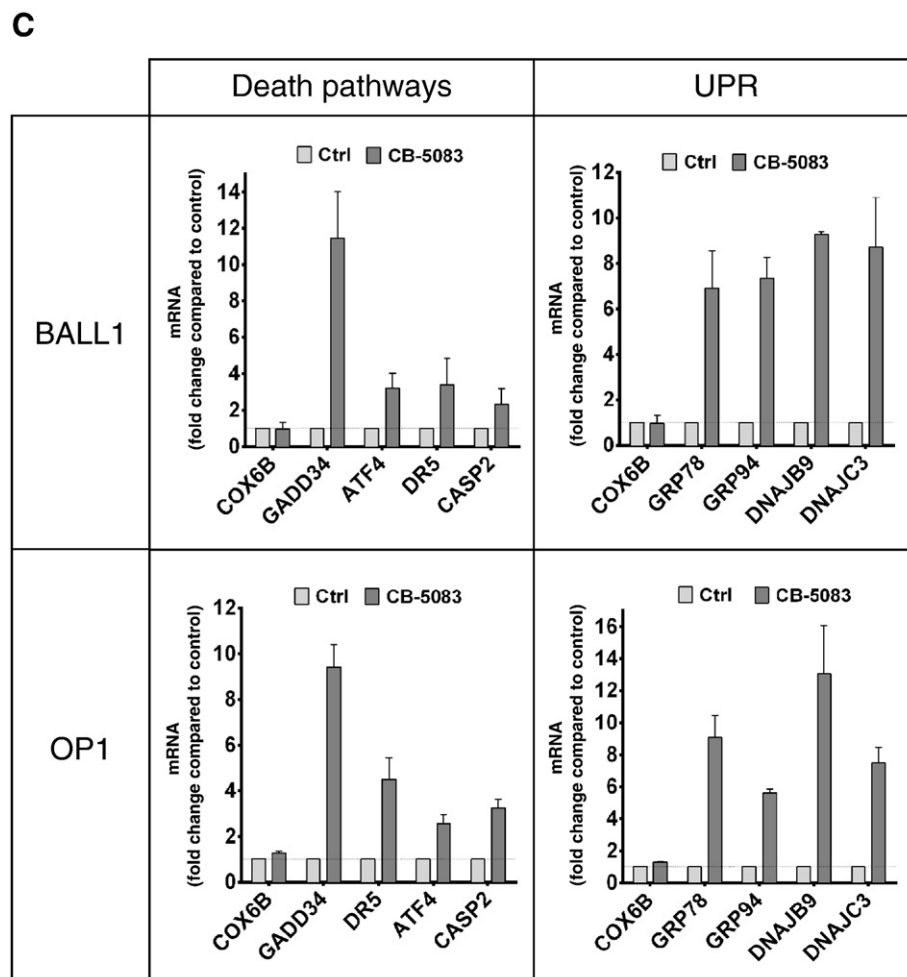


Figure 5. (continued.)

antileukemic activity in B-ALL cell lines through the induction of a severe ER stress. Indeed, the ER stress was documented through: 1) prominent expression of the chaperones (GRP78, GRP94, PDI, DNAJC3, and DNAJB9); 2) increased activation of IRE1- $\alpha$ , as demonstrated by prominent splicing of XBP1; and 3) activation of PERK resulting in significant overexpression of CHOP and its downstream genes (particularly GADD34 and DR5).

We showed that the knockdown of either of the chaperones GRP78 or GRP94 did not modify the sensitivity of B-ALL cells to CB-5083. This suggests that their overexpression following CB-5083 treatment is simply a marker of ER stress induction and that GRP78 and GRP94 do not have a major role in mediating CB-5083 cytotoxicity in B-ALL cells. This is congruent with the finding that silencing of GRP78 (shRNA) did not significantly affect the sensitivity to CB-5083 against colon cancer cell lines [15].

In contrast, we showed that the absence of XBP1 increased the sensitivity to CB-5083, suggesting that the XBP1 splicing counteracts the activity of CB-5083, probably mitigating the ER stress. Moreover, it was previously noted that deletion of XBP1 is associated with a compensatory IRE1- $\alpha$  hyperphosphorylation [21,22], possibly leading to increased and sustained RIDD (regulated IRE1-dependent decay) that promotes apoptosis [23,24]. Therefore, we may hypothesize that modulation of RIDD is relevant in mediating CB-5083 cytotoxicity. This could explain why CB-5083 and the

IRE1- $\alpha$  inhibitor HNA were not synergistic under severe ER stress induced by CB-5083. Inhibition of RIDD could have detrimental effects (decreased proapoptotic signaling) that overcome the benefits (increased ER stress) of XBP1 splicing inhibition.

Finally, vincristine was synergistic with CB-5083 with combination indexes [25] as low as 0.56 and 0.58 for BALL1 and OP1 cells, respectively. Vincristine mainly acts by blocking cell division. Perhaps vincristine kills cells that, despite their inhibition of p97, are able to progress from G1 to the S and G2/M phase. In contrast, even though high p97-VCP expression is correlated with a poor prednisone response in B-ALL [18], the inhibition of p97 with CB-5083 did not restore prednisolone sensitivity in prednisolone-resistant cell lines (BALL1 and REH), and the combination was not synergistic. Moreover, bortezomib, a proteasome inhibitor that causes ER stress, was not synergistic with CB-5083.

## Conclusions

CB-5083, an orally bioavailable p97 inhibitor, has significant activity against a diverse panel of B-ALL cell lines, regardless of their genetic alterations. The drug causes a severe ER stress, inducing apoptosis mainly through the PERK-CHOP axis. A potentially useful synergy with vincristine, a backbone of ALL therapy, was discovered. Targeting of VCP/p97 is a novel promising therapeutic approach in B-ALL with high-risk features.

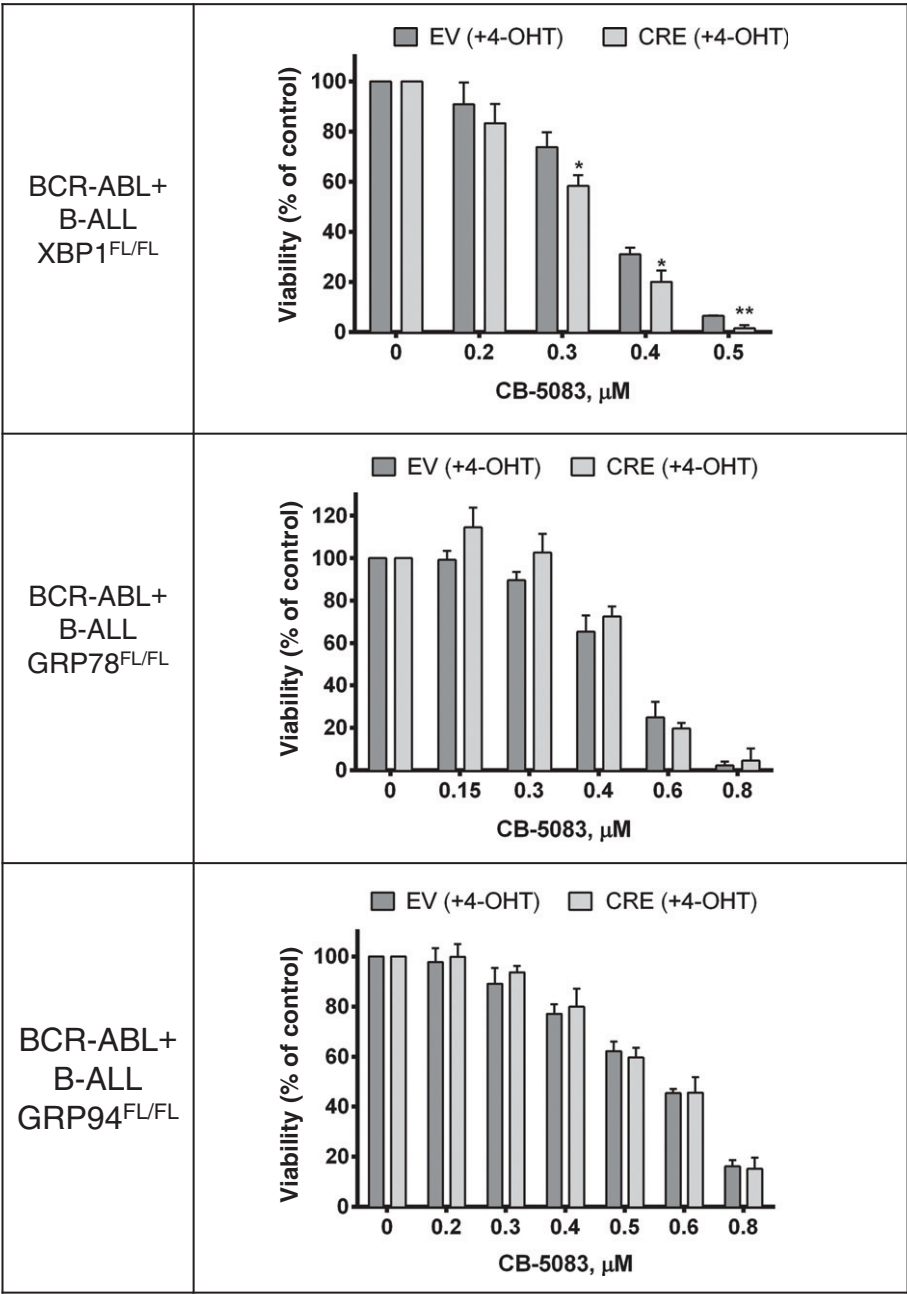


**Figure 6.** CB-5083 activity in GRP78, GRP94, and XBP1 knockdown models of BCR-ABL+ ALL.BCR-ABL+ B-ALL cells with floxed alleles (either GRP78<sup>FL/FL</sup>, GRP94<sup>FL/FL</sup>, or XBP1<sup>FL/FL</sup>), transfected with either empty vector (EV) or CRE recombinase, inducible with 4-hydroxy-tamoxifen (4-OHT), treated for 72 hours with 4-OHT 1  $\mu$ M and CB-5083 at different concentrations; viability was measured by MTT assays. Bar graphs represent mean  $\pm$  SD of three experiments, each in triplicates. \*:  $P < .05$ ; \*\*:  $P < .01$ .

Authors Contribution

G.G. and H.P.K. designed the study and wrote the manuscript; M.S., Q.C., D.L., H.S., S.T., S.G., R.L.M., M.R., M.M., and M.C. provided essential materials/reagents; G.G. performed the experiments and analyzed data; G.G., Q.C., D.L., S.G., and H.P.K. discussed the data; all authors reviewed and approved the final version of the manuscript.

Acknowledgements

We thank the Melamed Family and Reuben Yeroushalmi for their generous support. This research was supported by the National

Research Foundation Singapore under its Singapore Translational Research (STaR) Investigator Award (NMRC/STaR/0021/2014) and administered by the Singapore Ministry of Health's National Medical Research Council (NMRC), the NMRC Centre Grant awarded to National University Cancer Institute of Singapore, the National Research Foundation Singapore and the Singapore Ministry of Education under its Research Centres of Excellence initiatives. This work was also funded by the Leukemia Lymphoma Society of America and by the University of Bologna, Italy. This paper is dedicated to the memory of Parker Hughes.



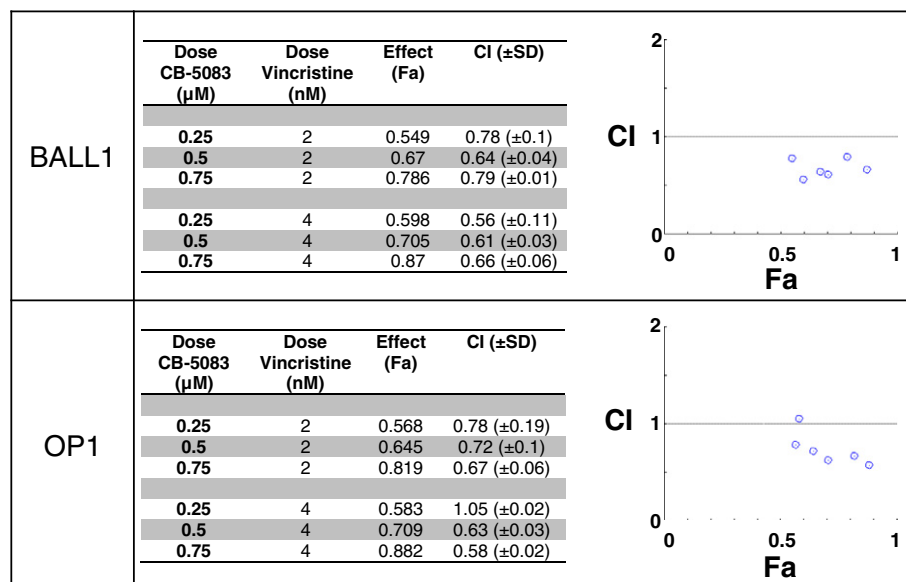


**Figure 7.** Synergistic activity of CB-5083 and vincristine. BALL1 and OP1 cells were treated for 24 hours with a combination of different concentrations of CB-5083 (0.25, 0.5, and 0.75 μM) and vincristine (2 and 4 nM). Viability was measured by MTT ( $n = 3$ ; each in triplicates). Fractional inhibition (Fa) is defined as the reduction of viability in treated cells compared to controls (Fa = 0, no inhibition; Fa = 1, complete inhibition). Combination index (CI) < 1 represents synergistic activity; = 1, additive effect. Right panels: CI and Fa for each combination tested.

## Appendix A. Supplementary data

Supplementary data to this article can be found online at <http://dx.doi.org/10.1016/j.neo.2017.08.001>.

## References

- [1] Hunger SP and Mullighan CG (2015). Acute lymphoblastic leukemia in children. *N Engl J Med* **373**, 1541–1552.
- [2] Inaba H, Greaves M, and Mullighan CG (2013). Acute lymphoblastic leukaemia. *Lancet* **381**, 1943–1955.
- [3] Curran E and Stock W (2015). How I treat acute lymphoblastic leukemia in older adolescents and young adults. *Blood* **125**, 3702–3710.
- [4] Rowe JM, Buck G, Burnett AK, Chopra R, Wiernik PH, Richards SM, Lazarus HM, Franklin IM, Litzow MR, and Ciobanu N, et al (2005). Induction therapy for adults with acute lymphoblastic leukemia: results of more than 1500 patients from the international ALL trial: MRC UKALL XII/ECOG E2993. *Blood* **106**, 3760–3767.
- [5] Muschen M (2015). Rationale for targeting the pre-B-cell receptor signaling pathway in acute lymphoblastic leukemia. *Blood* **125**, 3688–3693.
- [6] Kharabi Masouleh B, Geng H, Hurtz C, Chan LN, Logan AC, Chang MS, Huang C, Swaminathan S, Sun H, and Paietta E, et al (2014). Mechanistic rationale for targeting the unfolded protein response in pre-B acute lymphoblastic leukemia. *Proc Natl Acad Sci U S A* **111**, E2219–2228.
- [7] Sun H, Lin DC, Guo X, Kharabi Masouleh B, Gery S, Cao Q, Alkan S, Ikezoe T, Akiba C, and Paquette R, et al (2016). Inhibition of IRE1α-driven pro-survival pathways is a promising therapeutic application in acute myeloid leukemia. *Oncotarget* **7**, 18736–18749.
- [8] Meusser B, Hirsch C, Jarosch E, and Sommer T (2005). ERAD: the long road to destruction. *Nat Cell Biol* **7**, 766–772.
- [9] Sano R and Reed JC (2013). ER stress-induced cell death mechanisms. *Biochim Biophys Acta* **1833**, 3460–3470.
- [10] Pleasure IT, Black MM, and Keen JH (1993). Valosin-containing protein, VCP, is a ubiquitous clathrin-binding protein. *Nature* **365**, 459–462.
- [11] Sasset L, Petris G, Cesaratto F, and Burrone OR (2015). The VCP/p97 and YOD1 proteins have different substrate-dependent activities in endoplasmic reticulum-associated degradation (ERAD). *J Biol Chem* **290**, 28175–28188.
- [12] Meyer H, Bug M, and Bremer S (2012). Emerging functions of the VCP/p97 AAA-ATPase in the ubiquitin system. *Nat Cell Biol* **14**, 117–123.
- [13] Meyer H and Wehl CC (2014). The VCP/p97 system at a glance: connecting cellular function to disease pathogenesis. *J Cell Sci* **127**, 3877–3883.
- [14] Magnaghi P, D'Alessio R, Valsasina B, Avanzi N, Rizzi S, Asa D, Gasparri F, Cozzi L, Cucchi U, and Orrenius C, et al (2013). Covalent and allosteric inhibitors of the ATPase VCP/p97 induce cancer cell death. *Nat Chem Biol* **9**, 548–556.
- [15] Anderson DJ, Le Moigne R, Djakovic S, Kumar B, Rice J, Wong S, Wang J, Yao B, Valle E, and Kiss von Soly S, et al (2015). Targeting the AAA ATPase p97 as an approach to treat cancer through disruption of protein homeostasis. *Cancer Cell* **28**, 653–665.
- [16] Zhou HJ, Wang J, Yao B, Wong S, Djakovic S, Kumar B, Rice J, Valle E, Soriano F, and Menon MK, et al (2015). Discovery of a first-in-class, potent, selective, and orally bioavailable inhibitor of the p97 AAA ATPase (CB-5083). *J Med Chem* **58**, 9480–9497.
- [17] Moorman AV (2016). New and emerging prognostic and predictive genetic biomarkers in B-cell precursor acute lymphoblastic leukemia. *Haematologica* **101**, 407–416.
- [18] Lauten M, Schrauder A, Kardinal C, Harbott J, Welte K, Schlegelberger B, Schrappe M, and von Neuhoff N (2006). Unsupervised proteome analysis of human leukaemia cells identifies the Valosin-containing protein as a putative marker for glucocorticoid resistance. *Leukemia* **20**, 820–826.
- [19] Iritani BM and Eisenman RN (1999). c-Myc enhances protein synthesis and cell size during B lymphocyte development. *Proc Natl Acad Sci U S A* **96**, 13180–13185.
- [20] Hart LS, Cunningham JT, Datta T, Dey S, Tameire F, Lehman SL, Qiu B, Zhang H, Cerniglia G, and Bi M, et al (2012). ER stress-mediated autophagy promotes Myc-dependent transformation and tumor growth. *J Clin Invest* **122**, 4621–4634.
- [21] Lu M, Lawrence DA, Marsters S, Acosta-Alvear D, Kimmig P, Mendez AS, Paton AW, Paton JC, Walter P, and Ashkenazi A (2014). Cell death. Opposing unfolded-protein-response signals converge on death receptor 5 to control apoptosis. *Science* **345**, 98–101.
- [22] Niederreiter L, Fritz TM, Adolph TE, Krismer AM, Offner FA, Tschurtschenthaler M, Flak MB, Hosomi S, Tomczak MF, and Kaneider NC, et al (2013). ER stress transcription factor Xbp1 suppresses intestinal tumorigenesis and directs intestinal stem cells. *J Exp Med* **210**, 2041–2056.
- [23] Han D, Lerner AG, Vande Walle L, Upton JP, Xu W, Hagen A, Backes BJ, Oakes SA, and Papa FR (2009). IRE1α kinase activation modes control alternate endoribonuclease outputs to determine divergent cell fates. *Cell* **138**, 562–575.
- [24] Maurel M, Chevet E, Tavernier J, and Gerlo S (2014). Getting RIDD of RNA: IRE1 in cell fate regulation. *Trends Biochem Sci* **39**, 245–254.
- [25] Chou TC (2010). Drug combination studies and their synergy quantification using the Chou-Talalay method. *Cancer Res* **70**, 440–446.